SUPPORTING INFORMATION

Na_3FeH_7 and Na_3CoH_6: Hydrogen-rich first-row transition metal hydrides from high pressure synthesis

Kristina Spektor,[1,*] Wilson A. Crichton,[1] Stanislav Filippov,[2,3] Sergei I. Simak,[2] Andreas Fischer,[4] and Ulrich Häussermann[3,*]

[1] *ESRF, The European Synchrotron Radiation Facility, F-38000 Grenoble, France*

[2]*Theoretical Physics Division, Department of Physics, Chemistry and Biology (IFM) Linköping University, SE-581 83, Linköping, Sweden*

[3]*Department of Materials and Environmental Chemistry, Stockholm University, SE-10691 Stockholm, Sweden*

[4]*Department of Physics, Augsburg University, D-86135 Augsburg, Germany*

*E-mails: Kristina.Spektor@gmail.com

Ulrich.Haussermann@mmk.su.se

Detailed description of in situ high pressure experiments

Structural investigations and refinement strategies used for *LP* and *HT-HP* $Na_3(TM)H_n$ compounds (TM = Fe, Co)

Detailed description of results from theoretical calculations

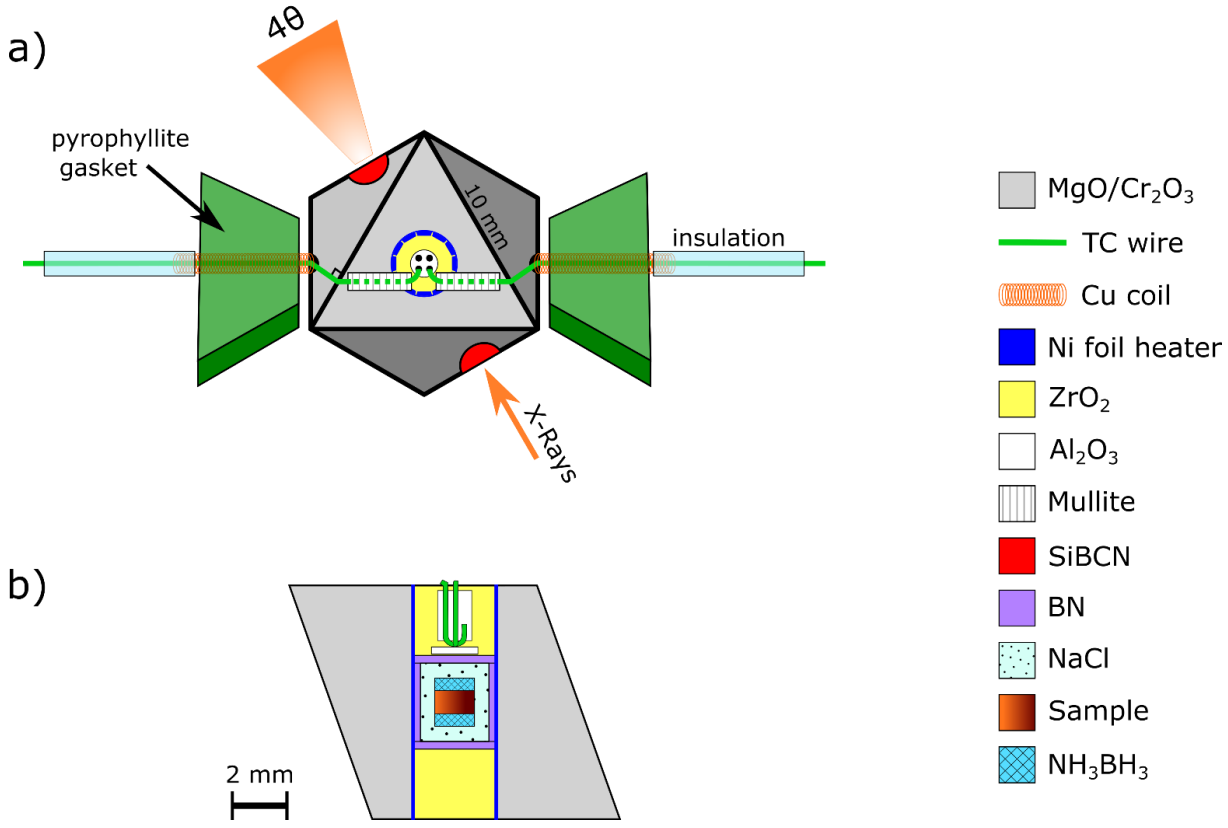

Figure S1. Sketch of the 10/5 multianvil assembly with a type C thermocouple (TC) included. (a) Positioning of the filled octahedron with the TC relative to the X-ray beam. (b) Arrangement of the sample and the TC inside the assembly.

DETAILED DESCRIPTION OF IN SITU HIGH PRESSURE EXPERIMENTS

1. Compression

Both Na–TM–H (TM = Fe, Co) samples were compressed to the target pressure of ~10 GPa using the large volume press at ID06-LVP, ESRF.[1] For the first ~25 min the samples were pressurized at a lower rate (2.6–2.9 GPa/h), while further compression was performed at 3.3–3.5 GPa/h. At the end of the compression (which corresponded to 170 bar oil pressure) the pressure was estimated as ~10.3 GPa for both samples. The compression was followed by heating, and the detailed descriptions of changes in the PXRD patterns at increased temperatures are provided below for each Na–TM–H system.

2. Heating of Na–Fe–H system at ~10 GPa

Temperature variations during the heating of the 2NaH:1Fe sample at ~10.3 GPa are shown in Figure S2. The heating was commenced at a rate of 4–6 °C/min, which was slowly increased to 9–12 °C/min above ~110 °C. At around 210 °C, formation of *hcp*-FeH_x hydride was noted in the PXRD patterns. This indicated that the release of hydrogen from ammonia borane (NH_3BH_3) source was in progress. During the ~10 min temperature dwell at ~ 250 °C a new set of very faint reflections appeared in the diffraction patterns, manifesting the formation of a ternary high pressure, high temperature Na–Fe–H phase further denoted as *HT-HP* Na_3FeH_7 (see also Figure 1a in the main text). The heating was then continued at a gradually decreasing rate (from 8 to 5 °C/min) until the temperature reached 390 °C. At this point H_2 release from the source was expected to be completed,[2] and the temperature was kept constant for ~45 min to observe the development of the new phase. The intensity of the new peaks significantly increased upon the described temperature variations, and the reflections were indexed to a face-centered cubic cell with $a \approx 7.1$ Å at 390 °C and ~10 GPa. To aid the completion of the *HT-HP* Na_3FeH_7 formation the sample was slowly heated further to ~470 °C (at 4–5 °C/min) in ~15 °C steps alternating with temperature dwells. At ~440 and 470 °C the sample was dwelled for ~1 h 40 min and ~40 min, respectively. PXRD data collected during the 440 °C dwell was later used for the Rietveld refinements of the *HT-HP* phase. Interestingly, iron hydride at these temperatures appeared to be a mixture of *fcc*- and *dhcp*-FeH_x, as well as *hcp*-FeH_x with a low H content.[3,4] It is not clear what caused this complex behavior of iron hydrides, but it could be related to complexity of the multiphase system. The sample was subsequently slowly cooled down to 120 °C (at 8–12 °C/min) in order to explore possible temperature-induced phase transitions of the *HT-HP* phase. At ~145 °C a set of additional, extremely weak, peaks appeared in the pattern (see Figure 1a) while the original *HT-HP* peaks did not change significantly, apart from showing tiny and rapid shifts towards higher 2θ angles. The presence of the additional peaks was interpreted as a transformation of *HT-HP* Na_3FeH_7 into a low temperature, high pressure phase, further noted as *LT-HP* I. After a ~25 min dwell at ~120 °C the sample was reheated to 170 °C (at 8 °C/min). The

observed changes were entirely reverted at ~150 °C, implying the back-transformation to *HT-HP* phase. At 170 °C the temperature was quenched by turning off the controller. Rapid cooling did not preserve the *HT-HP* phase – instead, another set of faint peaks different from those observed below 150 °C instantly appeared in the pattern, suggesting the transformation into a second low temperature, high pressure form *LT-HP* II. The cell parameter *a* of *HT-HP* Na_3FeH_7 varied between 7.08 and 7.12 Å during the course of heating. The estimated pressure after the quench was ~8.7 GPa.

To investigate the phase relations between the *HP* Na_3FeH_7 polymorphs further, after the temperature quench the sample was carefully reheated to ~200 °C and then slowly cooled to RT (at 5–7 °C/min). The changes observed in the PXRD patterns during the heating-cooling cycle are shown in detail in Figure S3. The *LT-HP* II phase transforms instantly into *LT-HP* I Na_3FeH_7 at ~105 °C on heating, as the respective sets of the additional peaks replace one another (Figure S3a). *LT-HP* I peaks disappear around 150 °C as the transition to the *HT-HP* form occurs. On cooling the transformations appear completely reversible and are as rapid as on heating, with only a slight temperature hysteresis: *HT-HP* → *LT-HP* I transition is seen at ~145 °C, and *LT-HP* I → LT-HP II at ~90 °C. Inspection of high angle data again revealed very minor, but noticeable instantaneous shifts of the original *HT-HP* reflections, as well as slight broadening, which occurred simultaneously with the appearance of *LT-HP* I/II peaks (Figure S3b). Inspecting closely the peaks related to *LT-HP* I, II phases revealed that the small additional reflections could not be obtained at given 2θ angles by any direct symmetry lowering of the *HT-HP* cubic cell. Since molecular dynamics simulations suggested reorientational dynamics of FeH_7^{3-} complexes in *HT-HP* Na_3FeH_7, both *LT-HP* phases likely represent superstructures arising from the ordering of $(TM)H_n^{3-}$ complexes. It was not possible to extract the unit cell parameters of the *LT-HP* phases from in situ PXRD due to significant peak overlap along with extremely low intensity of the possible superstructure reflections. The behavior seems to be similar to Na_3NiH_5, possessing square pyramidal NiH_5^{3-} complexes; however, the structure of the *LT-HP* phase could be solved from similar data.[5] It can be assumed that the superstructures account for slight distortions of the Na^+ counterion environment around complexes.

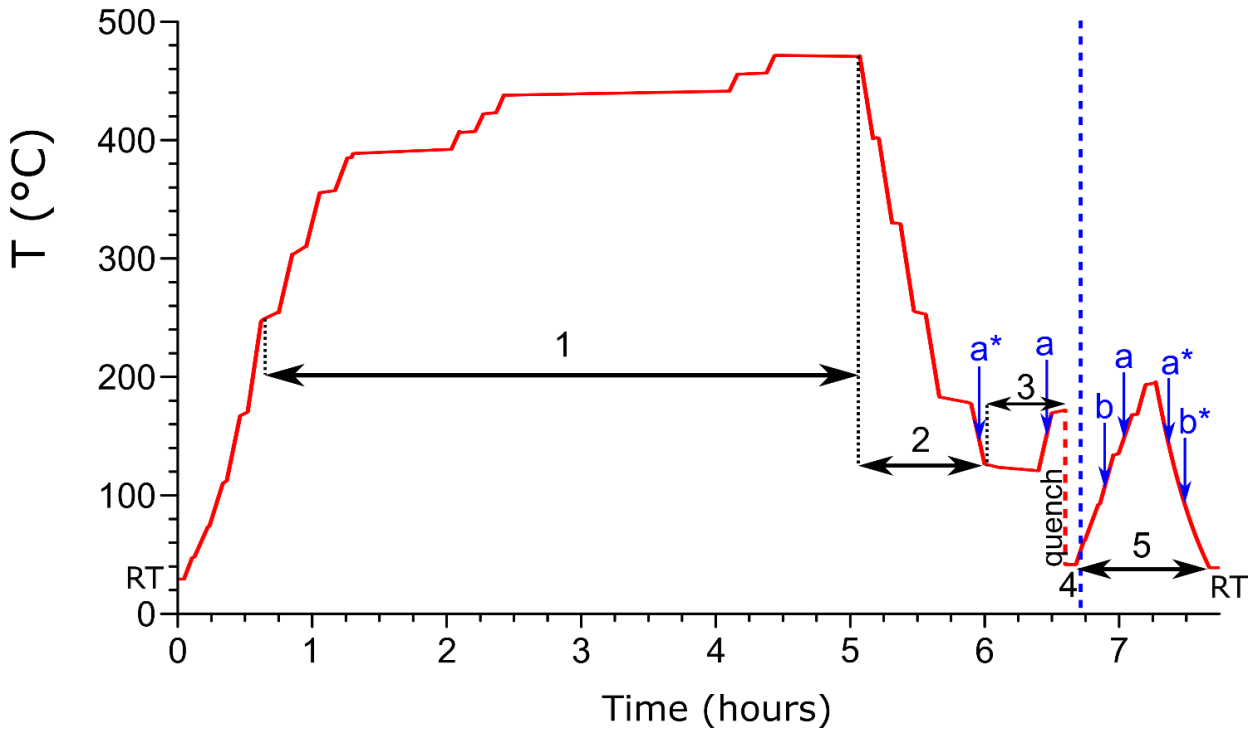

Figure S2. Temperature variations as a function of time during the PXRD in situ study of the Na–Fe–H system (starting pressure ~10 GPa). Numbers refer to the following stages of the experiment: (1) formation and growth of *HT-HP* Na_3FeH_7 on heating; (2) cooling down and transition of *HT-HP* to the *LT-HP* I phase; (3) reheating and transformation back to the *HT-HP* phase; (4) temperature quench accompanied by instant *HT-HP* transition to *LT-HP II* phase; (5) slow reheating and cooling cycle where Na_3FeH_7 follows *LT-HP* II → *LT-HP* I → *HT-HP* transformation sequence on heating, and on cooling the sequence is reversed (see also Figure S3). The blue dashed line corresponds to the end of Figure 1a in the main text. Blue arrows and letters mark the phase transitions on heating: (a) *LT-HP* I → *HT-HP*, (b) *LT-HP* II → *LT-HP* I; reversed transitions on cooling are noted with asterisks.

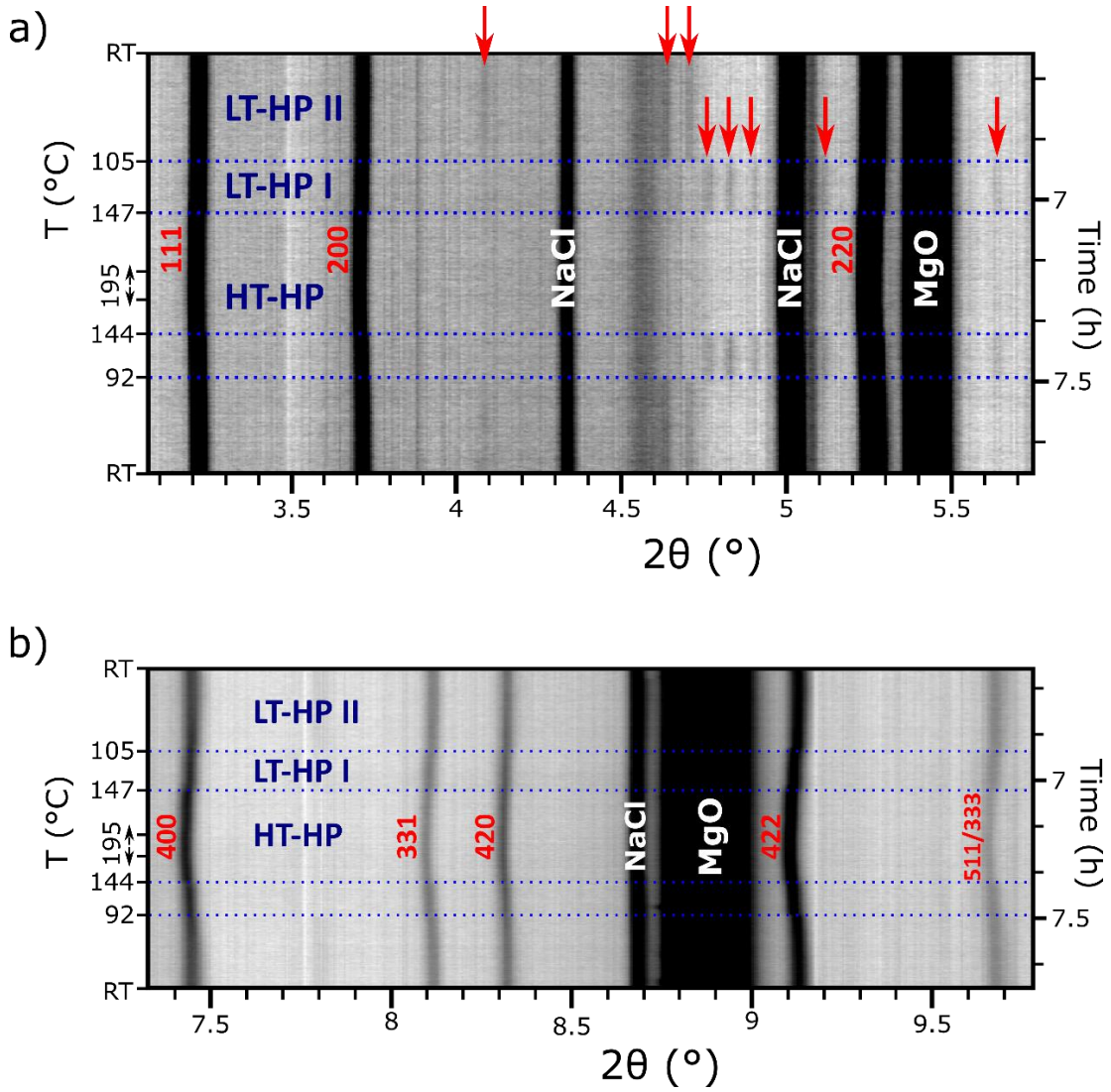

Figure S3. Close ups of different 2θ ranges of the same compilation of in situ PXRD patterns (λ = 0.2296 Å) collected during the heating-cooling cycle at the end of the Na–Fe–H experiment (labeled "5" in Figure S2). The changes occurring during the *LT-HP* II→*LT-HP* I→*HT-HP* phase transitions are shown (note that all transitions are reversible on heating and cooling): (a) sets of additional peaks at low angles characteristic for *LT-HP* I and II phases (marked with red arrows); (b) slight shifts and broadening in *HT-HP* peak positions, visible at higher 2θ angles, accompany the phase transitions. Indices of the *HT-HP* phase reflections are shown in red, and blue dotted lines mark the onsets of the phase transitions. The diffraction intensities are shown on the logarithmic scale to enhance signal-to-noise ratio for the low intensity reflections.

3. Heating of Na–Co–H system at ~10 GPa

Temperature variations during the heating of the 2NaH:1Co sample at ~10.3 GPa are shown in Figure S4. The heating was initiated at a rate of 3 °C/min, which was gradually increased to 9 °C/min by 170 °C. Above 150 °C diffuse peaks started to develop at the lower 2θ angles of *hcp*-Co diffraction peaks, which was attributed to the formation of *hcp*-CoH_x and indicated that the H_2 release from the NH_3BH_3 source has started. During the ~10 min temperature dwell at 170 °C a new set of extremely weak reflections started to emerge in PXRD patterns. As the heating was continued further (7–9 °C/min), the intensity of the new reflections increased rapidly (see Figure 1b in the main text). At 325 °C, the temperature was kept constant for 20 min in order to complete the hydrogen release from the source. At this point, and as in the Na–Fe–H system, the set of new peaks could be indexed to a face-centered cubic unit cell with $a \approx 7.01$ Å. This phase is referred as *HT-HP* Na_3CoH_6. To aid the formation of *HT-HP* Na_3CoH_6, the heating was resumed at a lower rate (~5 °C/min) and was performed in approx. 30 °C steps, alternating with <15 min dwells. The peaks of the *HT-HP* phase continued to increase their intensity with temperature, and active recrystallization was noted above 390 °C. At 420 °C, the temperature was held for about 1 hour. No significant changes were noted in the patterns, apart from the transition of *hcp*-CoH_x into its *fcc* form.[6,7] Following this, the sample was cooled slowly to ~165 °C (10–13 °C/min) in order to test the *HT-HP* Na_3CoH_6 for the possible temperature-induced phase transitions. Again, the resemblance to the Na–Fe–H system was noted as several very faint additional peaks appeared in PXRD patterns at 295 °C (see Figure 1b). Simultaneous changes occurred in the peaks of the *HT-HP* phase, manifesting in pronounced instant broadening of the reflections (Figure S5). These changes occurred rapidly and upon reheating to 350 °C (~15 °C/min), reverted completely with no evident hysteresis. The data collected during the ~20 min dwell at 350 °C was later used for the Rietveld refinement of *HT-HP* Na_3CoH_6. The observed events indicate a presence of a low-temperature, high pressure polymorph *LT-HP* Na_3CoH_6 that has lower symmetry than the *HT-HP* form. The transition temperature suggests that Na_3CoH_6 initially started to form as the *LT-HP* phase. Similar to the Fe analogue, *HT-HP* Na_3CoH_6 was expected to contain CoH_6^{3-} complexes that undergo reorientational dynamics. The rapid and reversible character of the *HT-HP* → *LT-HP* transformation suggests that it also likely occurs due to the arresting of dynamics of the CoH_6^{3-} ions. Again, it was not possible to obtain the additional peaks at 2θ positions as observed in the in situ PXRD via a direct symmetry lowering and the introduction of small distortions that would account for the peak broadening. We nonetheless consider it likely that the *LT-HP* polymorph is an ordered superstructure of the dynamically disordered *HT-HP* phase. More detailed analysis and indexing of the *LT-HP* unit cell were not feasible due to significant peak overlap in the in situ PXRD patterns and the extremely low intensities of possible superstructure reflections.

In order to check if some other phases can be accessed in the Na–Co–H system, the sample was heated back up to 400 °C (14–17 °C/min) and re-compressed (not shown in Figure 1b). The estimated pressure before re-compression was ~8.6 GPa, which was lower than at the start of the

experiment, and was increased back to ~9.6 GPa at ~0.8 GPa/h. No changes were noted during the compression, and the heating-cooling cycle was repeated once again to observe the *HT-HP* ↔ *LT-HP* transition (~19 °C/min). The estimated temperature for both direct and back-transformation was somewhat higher, at ~315 °C. However, the temperature could be slightly overestimated, as electrical resistance of the Ni heater decreases with pressure, and the temperature was derived from the calibration of thermocouple readings vs power during the Na–Fe–H run. The temperature was then quenched from 400 °C. Again, as in the Na–Fe–H experiment, the *HT-HP* phase was not preserved during the rapid cooling, but instantly converted to the *LT-HP* phase. Pressure after the quench corresponded to ~9.3 GPa. The cell parameter *a* of the *HT-HP* Na_3CoH_6 varied within ~7.00–7.05 Å during the experiment.

4. Decompression

After the heating was complete, the Na–TM–H samples were decompressed over the course of several hours. There were no changes observed in the PXRD patterns, apart from the lattice expansion. The estimated residual pressure at the end of decompression was 1.9 and 0.7 GPa for the Fe- and Co-containing samples, respectively. The samples were then recovered at ambient *p, T* in an argon-filled glove box. Approximately half of each product was loaded in a glass capillary as a single piece and used for ex situ characterization at ID15B, ESRF. Ex situ PXRD examination revealed that the *LT-HP* $Na_3(TM)H_n$ phases transformed almost completely into the low pressure polymorphs, *LP* Na_3FeH_7 and *LP* Na_3CoH_6. The 2D PXRD patterns collected at ID15B are shown in Figure S6. Details of the structural investigations and Rietveld refinements for the *LP* and *HT-HP* $Na_3(TM)H_n$ phases are provided in the next sections.

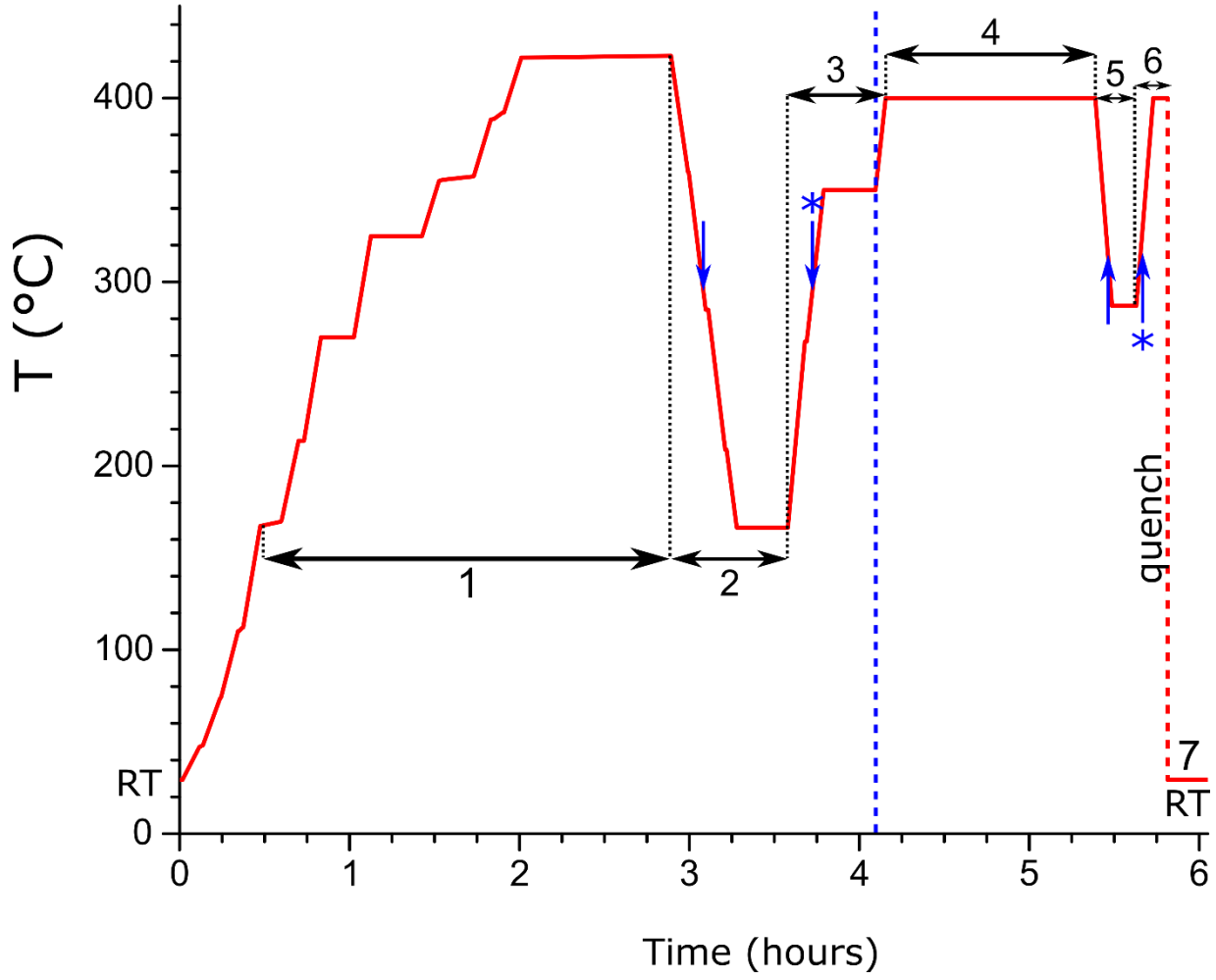

Figure S4. Temperature variations as a function of time during the PXRD in situ study of the Na–Co–H system (starting pressure ~10 GPa). Numbers refer to the following stages of the experiment: (1) formation and growth of Na_3CoH_6 phases on heating; *HT-HP* phase is expected to be stable above 300 °C; (2) cooling down and transition of *HT-HP* to the *LT-HP* polymorph; (3) reheating and reverse transformation to the *HT-HP* phase; (4) pressure increase from ~8.6 to ~9.6 GPa; (5), (6) cooling down and subsequent reheating (after recompression) during which *HT-HP* transforms to *LT-HP* and back; (7) temperature quench and instant *HT-HP* → *LT-HP* transition. The blue dashed line corresponds to the end of Figure 1b in the main text. Blue arrows mark the *HT-HP* → *LT-HP* phase transitions on cooling; reversed transitions on heating are noted by arrows with asterisks.

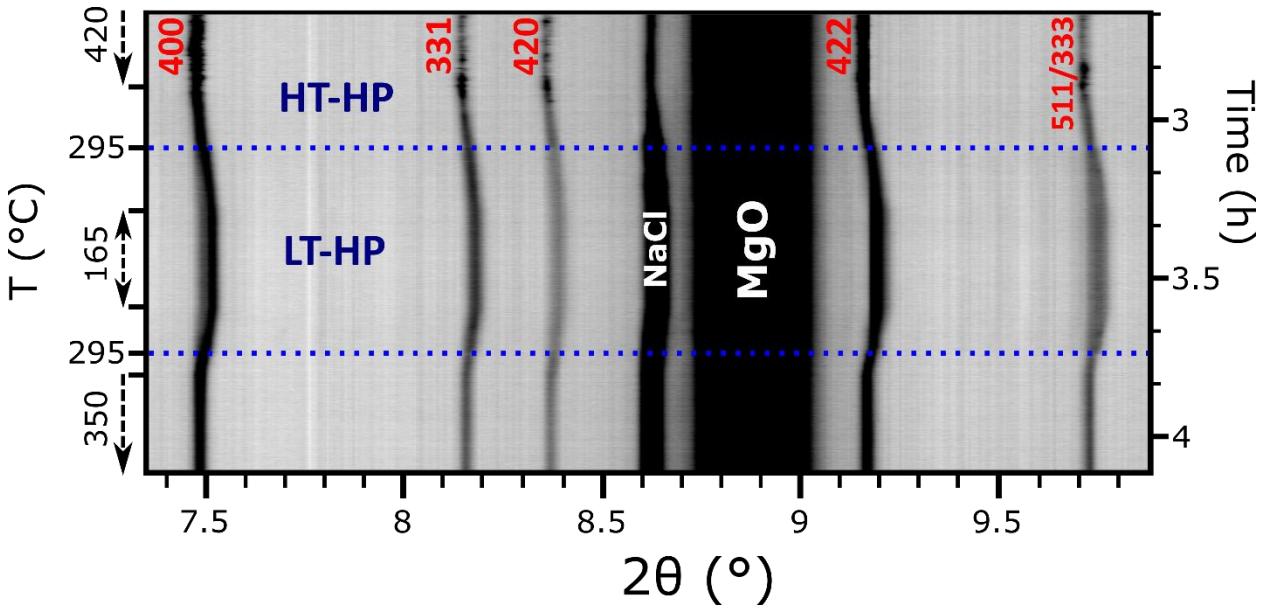

Figure S5. Magnified high 2θ angle range of the compiled in situ PXRD patterns (λ = 0.2296 Å) showing the changes during direct and reverse *HT-HP* ↔ *LT-HP* transformations of Na_3CoH_6 polymorphs on cooling and heating during the Na–Co–H experiment (labels "2" and "3" in Figure S4). Indices of the *HT-HP* phase reflections are shown in red, and blue dotted lines mark the onsets of the phase transitions. The peaks of the *HT-HP* phase clearly show broadening upon the transition to *LT-HP*, which occurs simultaneously with appearance of additional, weak peaks (see Figure 1b in the main text) and is entirely reversible during back-transformation to the *HT-HP* form.

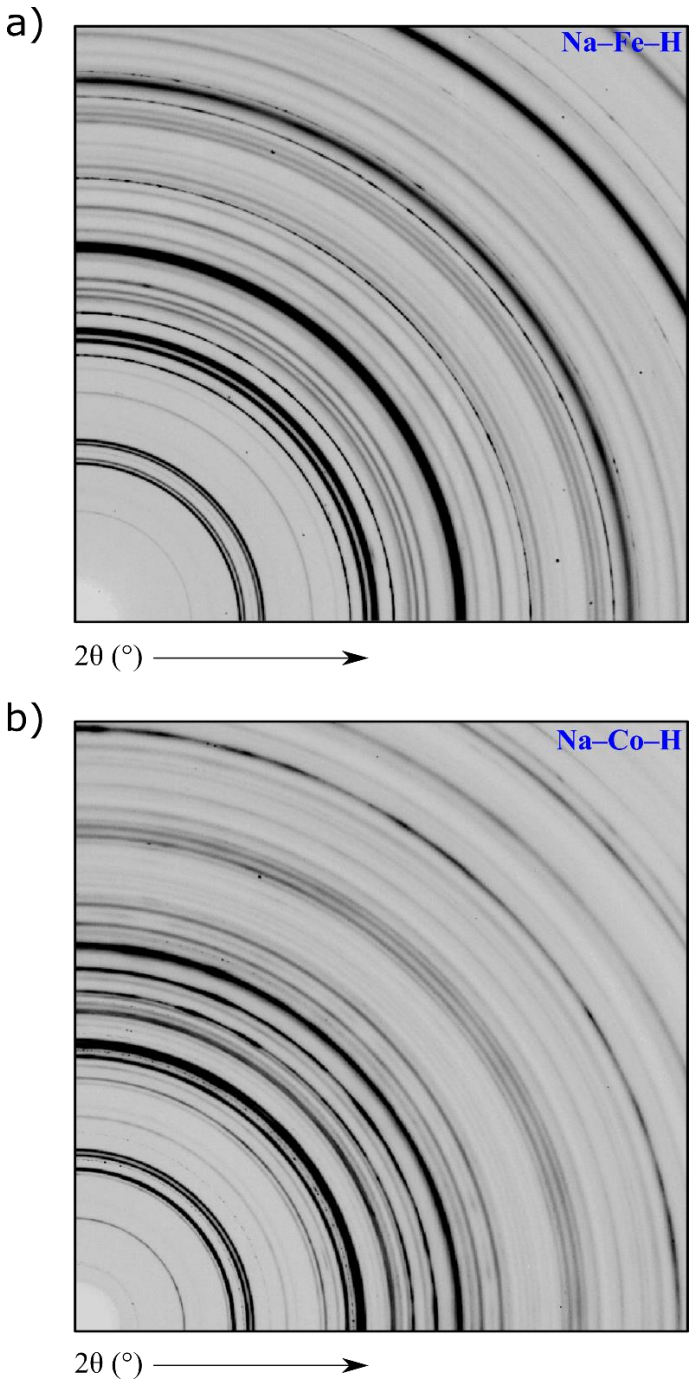

Figure S6. Segments of 2D PXRD patterns collected at ID15B, ESRF (λ= 0.41112 Å) for the products of Na–Fe–H (a) and Na–Co–H (b) runs at ambient *p, T*. The corresponding integrated 1D patterns were used for the structural studies of the *LP* $Na_3(TM)H_n$ (TM = Fe, Co). Both products contain the *LP* Na_3FeH_7 and Na_3CoH_6 phases as major ternary compounds, while the texture contribution to the patterns does not appear significant. In addition, the products contain leftover starting materials (NaH, *bcc*-Fe, *hcp*-Co) and trace amounts of untransformed *LT-HP* polymorph.

STRUCTURAL INVESTIGATIONS AND REFINEMENT STRATEGIES USED FOR *LP* AND *HT-HP* $Na_3(TM)H_n$ COMPOUNDS (TM = Fe, Co).

The integrated 2D PXRD data acquired at ID15B, ESRF were used for the structural investigations and refinements of both *LP* Na_3FeH_7 and Na_3CoH_6 products. Segments of respective 2D patterns are shown in Figure S6 (a,b). From examination of the PXRD patterns we identified that, apart from the peaks of leftover starting materials and trace amounts of *LT-HP* phases, each pattern contained a new set of reflections entirely different from those present at elevated pressures. The positions and intensities of these reflections strongly resembled those of already known $Na_3(Ru/Os)H_7$ and $Na_3(Rh/Ir)H_6$ complex hydrides,[8,9] strongly suggesting the existence of isostructural Na_3FeH_7 and Na_3CoH_6 phases.

To test the correctness of this suggestion, Le Bail analysis[10] was performed in Jana2006 software[11] using the space groups $P4_2/mnm$ (136) and *Pnma* (62) for the Fe- and Co-containing products, respectively. The chosen space groups corresponded to those of $Na_3(Ru/Os)H_7$ and $Na_3(Rh/Ir)H_6$ structures. To find the possible arrangements of Na and TM atoms in the structures, the extracted intensities were used for structure solution trials using the Superflip algorithm in Jana2006.[12] For both structures Superflip yielded a stable, reproducible solution with 3Na:1TM stoichiometry. The Wyckoff positions of the Na and TM (Fe, Co) atoms coincided with those in the $Na_3(Ru/Os)H_7$ and $Na_3(Rh/Ir)H_6$ structures, while their fractional coordinates were close as well. Rietveld refinements of the obtained arrangements against experimental data resulted in reasonable fits, strongly supporting the isostructural relations of *LP* $Na_3(TM)H_n$ products to $Na_3(Ru/Os)H_7$ and $Na_3(Rh/Ir)H_6$ compounds. Altogether with the proximity of cell parameters and volumes of *LP* Na-TM-H products and the known hydrides, this also suggests analogous content and arrangement of hydrogen atoms. The 3Na:1Fe and 3Na:1Co metal arrangements were further used for the DFT optimizations, along with hydrogen positions adapted from Ru/Os- and Rh/Ir-containing hydrides.

The DFT-optimized models of the *LP* Na_3FeH_7 and Na_3CoH_6 structures (Tables S1, S2) were used for final Rietveld refinements in Jana2006. In the case of the Na–Fe–H product, *bcc*-Fe and NaH phases were added to the refinement. In addition, residual *LT-HP* II Na_3FeH_7 phase was included in the refinement and fitted with an *fcc* unit cell (*Fm*-3*m*, space group 225) due to its low content. During the Na–Co–H product refinement *hcp*-Co phase was added to the fit, although some of its peaks were excluded along with those of residual *LT-HP* Na_3CoH_6. For both *LP* $Na_3(TM)H_n$ phases the Rietveld refinements followed the same strategy. The refined parameters included 6^{th} or 7^{th} degree polynomial background, the unit cell dimensions, components of pseudo-Voigt peak profile function, fractional coordinates and isotropic atomic displacement parameters (ADPs) of metal atoms. The ADPs of Na atoms were constrained together for the most part of the refinement, being released and refined separately only at the end. The fractional coordinates of H atoms (from DFT-optimized models) remained fixed during the fitting procedure along with their ADPs, which were kept at $U_{iso} = 0.038$ Å^2. The refinements demonstrated excellent fits of the DFT-optimized structures to the experimental PXRD data (R_{obs}

at 2.61 % and 2.3 % for Fe- and Co-containing structures, respectively). Resulting Rietveld plots are shown in Figure S7, and crystallographic data are presented in Tables S3,4.

Since the *LP* Na_3TMH_n structures were clearly established, the same 3Na:1TM stoichiometry of the metal arrangement was assumed for the *HT-HP* polymorphs. As the diffraction peaks of both polymorphs were indexed to a face-centered cubic unit cell, space group *Fm*-3*m* (225) was used for the Rietveld refinements. Along with the *fcc* lattice type, the unit cell dimensions and distribution of reflection intensities for both Fe- and Co-containing *HT-HP* phases clearly pointed at the isostructurality with the previously discovered *HT-HP* Na_3NiH_5.[5] Thus, an analogous Heusler-type structure was adapted for both phases, where Na atoms occupy 8*c* and 4*b* Wyckoff sites and Fe/Co atoms are placed at 4*a* sites. To account for the reorientational dynamics of FeH_7^{3-} and CoH_6^{3-} units, the H atoms in both structural models were placed at a 48*h* site (x = 0.15) with a site occupancy 7/12 or 6/12, respectively. The Rietveld refinements for *HT-HP* polymorphs were performed in Jana2006 using in situ PXRD data. The refinement procedures were practically the same for both *HT-HP* Na_3FeH_7 and Na_3CoH_6. The refined parameters included unit cell dimensions, components of a pseudo-Voigt peak profile function and isotropic ADPs of the metal atoms, while a manually created background was used during both refinements. The U_{iso} parameters of Na atoms were constrained together. The fractional coordinates of H atoms as well as their ADPs remained fixed during the refinement (U_{iso} = 0.038 $Å^2$). In addition, other phases were added to the refinements, such as NaH, NaCl and Fe/Co hydrides. Part of the NaCl peaks as well as reflections arising from the high pressure assembly (MgO, *h*-BN) were added to the excluded regions. The refinements yielded reasonable fits for both *HT-HP* Na_3FeH_7 and Na_3CoH_6, and the results are presented in Figure S8 as well as Tables S5-6. In addition, simulated patterns of the refined *HT-HP* phases are shown overlaid in Figure 1 in the main text (the cell parameters for the overlaid patterns are adjusted to the respective temperatures).

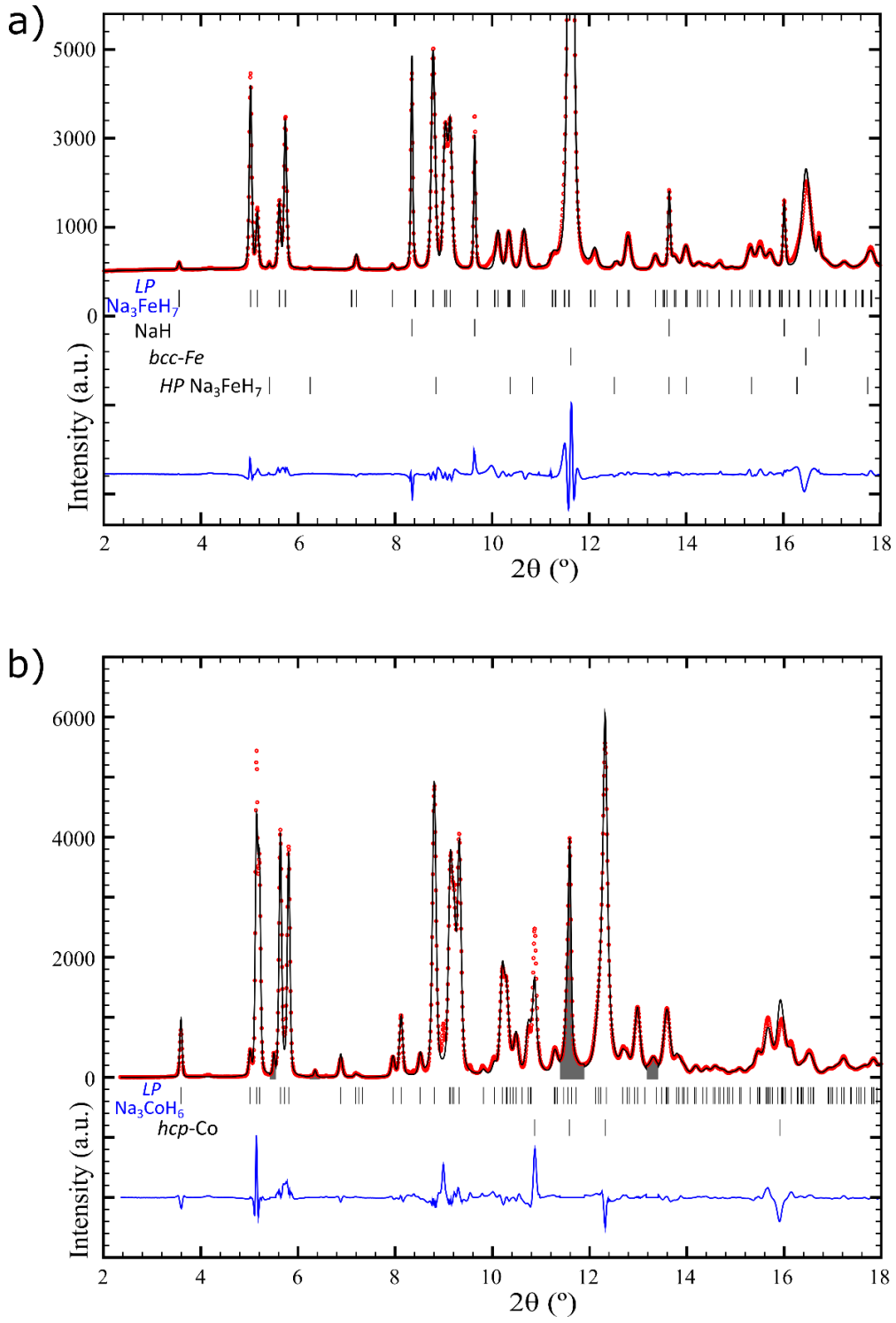

Figure S7. Rietveld fits of the DFT-optimized *LP* Na_3FeH_7 (a) and *LP* Na_3CoH_6 (b) structures to the ambient synchrotron PXRD data collected for the recovered products of Na–Fe–H and Na–Co–H experiments at ID15B, ESRF ($\lambda = 0.41112$ Å). Excluded regions are shown in grey.

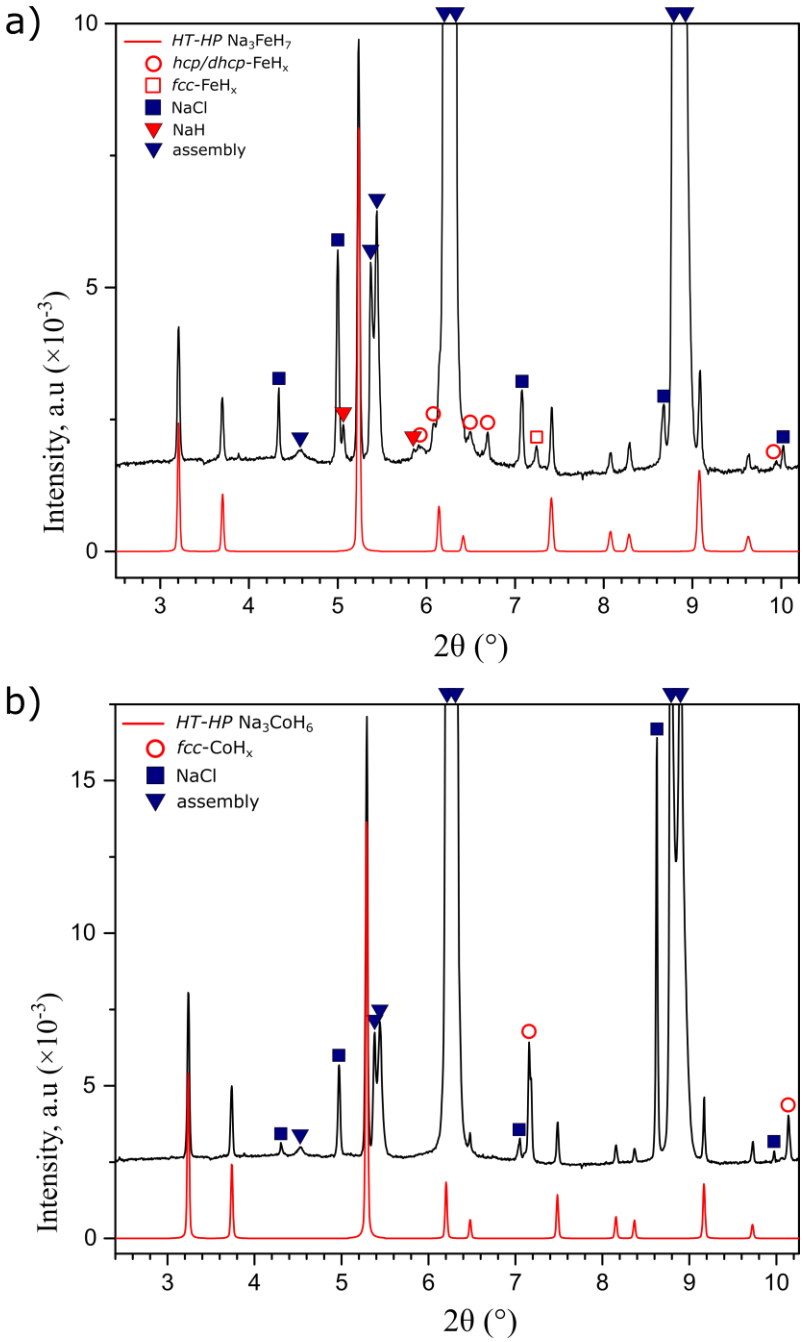

Figure S8. PXRD patterns of *HT-HP* Na_3FeH_7 (a) and Na_3CoH_6 (b), both shown in red, simulated from the results of Rietveld fit of the corresponding phases to the PXRD data (black) collected in situ at ID06-LVP, ESRF (λ = 0.2296 Å). The *p, T* conditions corresponded to ~10 GPa, 440 °C and ~8.6 GPa, 350 °C for the Fe- and Co-containing *HT-HP* phases, respectively. Diffraction peaks corresponding to assembly (MgO, *h*-BN) and part of NaCl reflections were excluded from the refinements.

Table S1. DFT-optimized structure of *LP* Na_3FeH_7 at ambient pressure (space group $P4_2/mnm$ (136), a = 9.3461 Å, c = 5.1154 Å, V = 446.83 Å^3).

Atom	***Wyck***	***x***	***y***	***z***
Fe	4*f*	0.2016	0.2016	0
Na1	8*i*	0.4669	0.8002	0
Na2	4*g*	0.1152	0.8848	0
H1	8*j*	0.1102	0.1102	0.1910
H2	8*j*	0.7591	0.7591	0.2799
H3	8*i*	0.3183	0.0736	0
H4	4*f*	0.6820	0.6820	0

Table S2. DFT-optimized *LP* Na_3CoH_6 structure at ambient pressure (space group *Pnma* (62), a = 9.0911 Å, b = 5.1030 Å, c = 9.3746 Å, V = 434.90 Å^3).

Atom	***Wyck***	***x***	***y***	***z***
Co	4*c*	0.2221	0.25	0.8993
Na1	4*c*	0.0442	0.25	0.6272
Na2	4*c*	0.8966	0.25	-0.0334
Na3	4*c*	0.2186	0.25	0.2501
H1	8*d*	0.3252	0.0315	-0.0395
H2	8*d*	0.1141	0.0415	0.8408
H3	4*c*	0.1323	0.25	0.0379
H4	4*c*	0.8065	0.25	0.7443

Table S3. Results of the Rietveld refinements of *LP* $Na_3(TM)H_n$ structures at ambient *p*, *T*.

Structure	*LP* Na_3FeH_7	*LP* Na_3CoH_6
Crystal system	Tetragonal	Orthorhombic
Space group	*P*4_2*/mnm* (136)	*Pnma* (62)
Z	4	4
Lattice parameters (Å)	*a* = 9.3839(4) *c* = 5.2267(4)	*a* = 9.1555(5) *b* = 5.1639(3) *c* = 9.3965(5)
V, $Å^3$	460.24(4)	444.25(4)
V/*Z* ($Å^3$ p.f.u)	115.06	111.06
Formula weight	131.87	133.95
$d_{calc}(g/cm^3)$	1.903	2.003
R_{obs} (%)	2.61	2.30
R_{all} (%)	2.61	2.30

Table S4. Fractional coordinates and atomic displacement parameters obtained from Rietveld refinement for *LP* $Na_3(TM)H_n$ structures at ambient *p, T*. Positions of H atoms corresponded to those in DFT-optimized structures and remained fixed during the refinement as well as their ADPs, which were set to U_{iso} = 0.038 Å^2.

atom	**site**	***x***	***y***	***z***	U_{iso} **(Å^2)**
***LP* Na_3FeH_7**					
Fe	4*f*	0.20328(18)	0.20328(18)	0	0.0191(11)
Na1	8*i*	0.4688(5)	0.7955(5)	0	0.0399(19)
Na2	4*g*	0.1162(4)	0.8838(4)	0	0.027(2)
***LP* Na_3CoH_6**					
Co	4*c*	0.2225(2)	0.25	0.8998(3)	0.0055(8)
Na1	4*c*	0.0461(6)	0.25	0.6278(6)	0.028(3)
Na2	4*c*	0.8956(6)	0.25	-0.0384(7)	0.028(2)
Na3	4*c*	0.2225(8)	0.25	0.2469(7)	0.028(3)

Table S5. Results of the Rietveld refinement of *HT-HP* $Na_3(TM)H_n$ structures at high *p, T* performed against in situ PXRD.

Structure	*HT-HP* Na_3FeH_7	*HT-HP* Na_3CoH_6
p, *T*	~10 GPa, 440 °C	~8.6 GPa, 350 °C
Crystal system	Cubic	Cubic
Space group	*Fm*-3*m* (225)	*Fm*-3*m* (225)
Z	4	4
Lattice parameters (Å)	*a* = 7.10708(16)	*a* = 7.03664(12)
V, Å^3	358.983(14)	348.414(10)
V/*Z* (Å^3 p.f.u)	89.746	87.104
Formula weight	131.88	133.95
d_{calc}(g/cm^3)	2.440	2.554
R_{obs} (%)	2.01	4.75
R_{all} (%)	2.01	4.75

Table S6. Fractional coordinates and atomic displacement parameters obtained from Rietveld refinement for *HT-HP* $Na_3(TM)H_n$ structures at high *p, T*. Hydrogen atoms were placed at a Wyckoff site 48*h* (*x* = 0.15) with an occupancy of 7/12 (*HT-HP* Na_3FeH_7) or 6/12 (*HT-HP* Na_3CoH_6) to create a dodecahedral ligand arrangement around TM atoms and thus account for the reorientational dynamics of FeH_7^{3-} and CoH_6^{3-} complex units. Positions of H atoms and their ADPs (U_{iso} = 0.038 Å^2) remained fixed during the refinement.

Atom	site	*x*	*y*	*z*	U_{iso} (Å^2)
***HT-HP* Na_3FeH_7 (~10 GPa, 440 °C)**					
Fe	4*a*	0	0	0	0.0087(16)
Na1	8*c*	0.25	0.25	0.25	0.053(2)
Na2	4*b*	0.5	0.5	0.5	0.053(2)
***HT-HP* Na_3CoH_6 (~8.6 GPa, 350 °C)**					
Co	4*a*	0	0	0	0.0578(16)
Na1	8*c*	0.25	0.25	0.25	0.123(2)
Na2	4*b*	0.5	0.5	0.5	0.123(2)

DETAILED DESCRIPTION OF REULTS FROM THEORETICAL CALCULATIONS

1. Total energy calculations

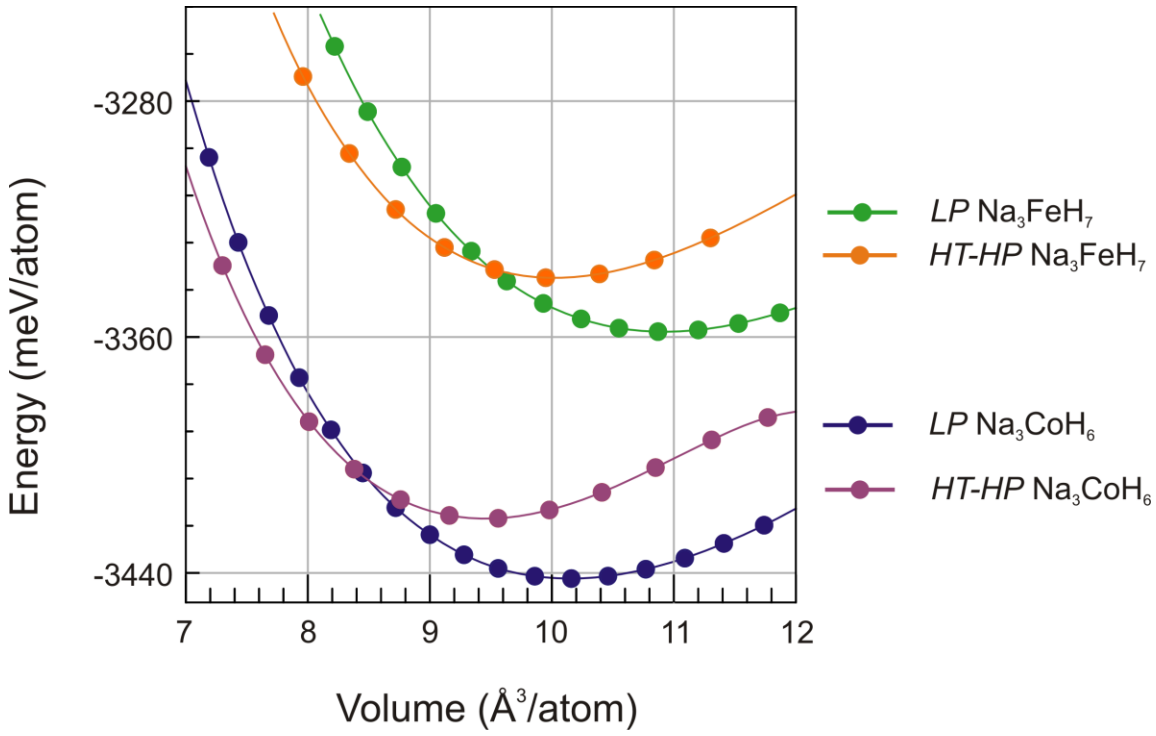

Figure S9: Total energy *vs* volume relations of pairs of *LP* and *HT-HP* $Na_3(TM)H_n$ phases (referring to zero K). The *HT-HP* models corresponded to an MD snapshot, which was relaxed in the considered volume range. The equilibrium volumes for *LP* and *HT-HP* Na_3FeH_7 are ~11 and ~10 $Å^3$/atom, respectively, and the ones for *LP* and *HT-HP* Na_3CoH_6 are ~10.2 and ~9.4 $Å^3$/atom, respectively.

2. Ab initio molecular dynamics simulations

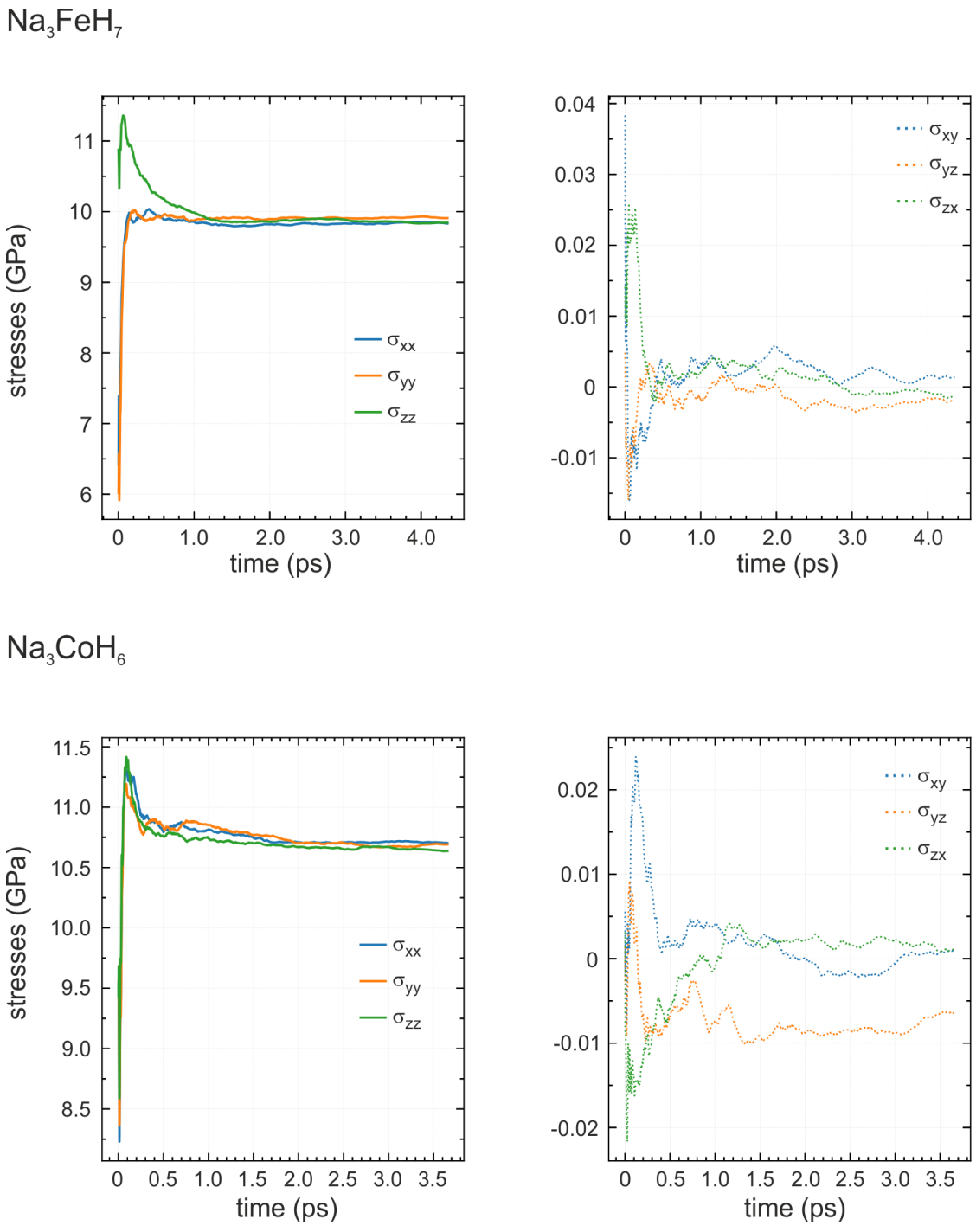

Figure S10: Diagonal (left panel) and non-diagonal components (right panel) of the Cauchy stress tensor as a function of the simulation time (1 time step = 1 ps) for *HT-HP* Na_3FeH_7 and Na_3CoH_6 at 1000 K.

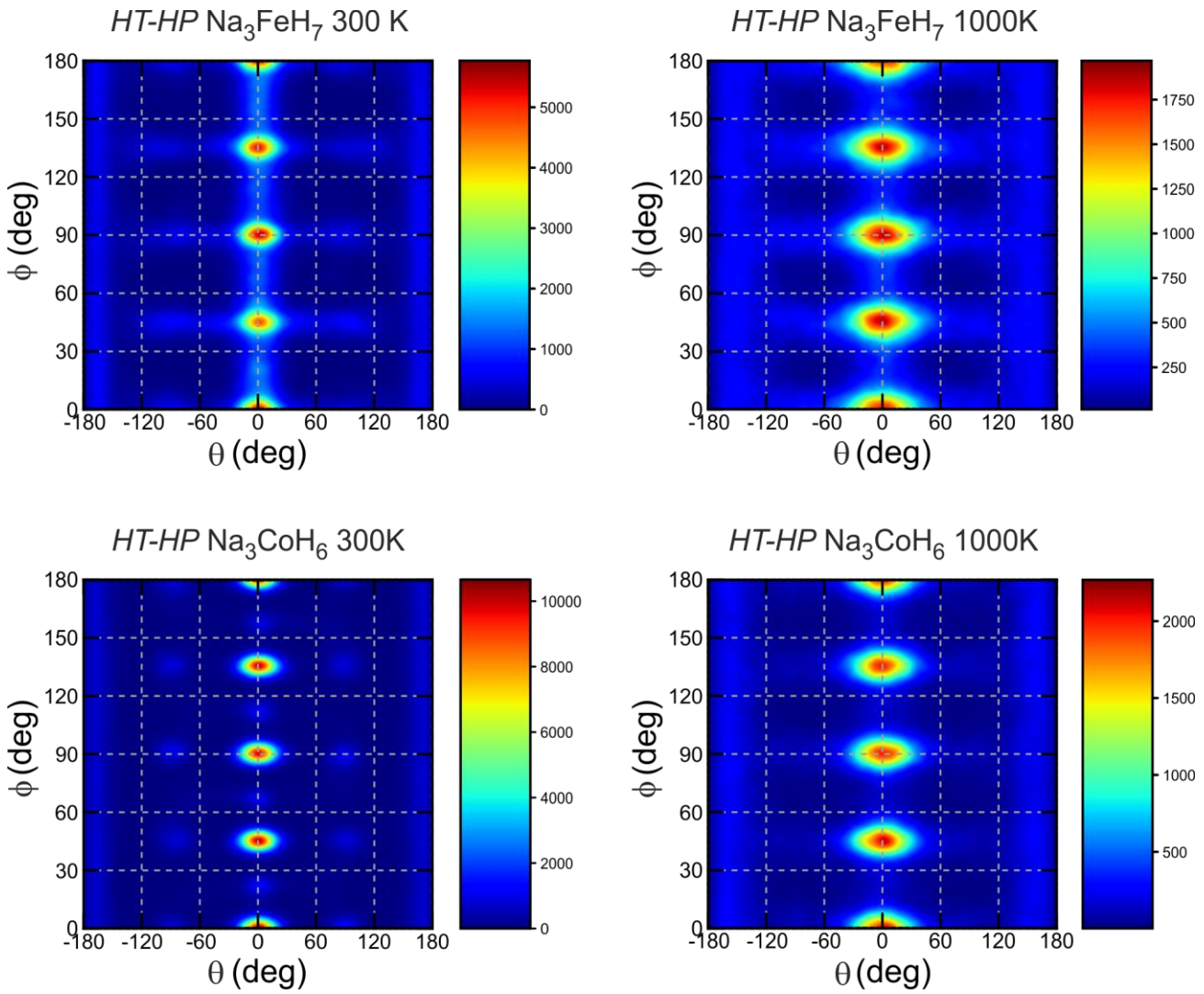

Figure S11: 2D histograms of angular positions of H atoms in the $(TM)H_n$ complexes for *HT-HP* Na_3FeH_7 and Na_3CoH_6 as obtained from AIMD simulations at 300 K (left hand panel) and 1000 K (right hand panel). The polar angle ϕ is defined as the angle between the z-axis of the simulation cell and the direction from TM to the H atom at $\mathbf{R}_i$. The azimuth θ is the angle between the projection of $\mathbf{R}_i$ on the xy-plane and the x-axis of the simulation cell. The angular pair (θ, ϕ) for each H atom in each $(TM)H_n$ complex at each time-step of the corresponding MD runs (except the equilibration period) was identified and added to the final dataset, which resulted in the 2D histograms shown above. Warmer colors (red, yellow, and light green) mean the frequent presence of H atoms at certain combinations of (θ, ϕ), whereas the coldest color (dark blue) means that these values were never observed. At 1000 K the H atoms of the complexes perform rotations, both with azimuthal and polar angles, which manifests itself in the presence of lighter coloured "bridges" between the spots. Reorientational dynamics seems to be present also for *HT-HP* Na_3FeH_7 at 300 K (lighter colored "bridges" between the spots) whereas

HT-HP Na_3CoH_6 at 300 K appears rather statically disordered (lighter coloured smaller spots). This coincides with the experimental observation that the *HT* to *LT* transition is at lower temperatures for Na_3FeH_7 (around 150 °C) compared to Na_3CoH_6 (around 300 °C).

This observation does not answer whether the dynamics is a rotation of the complex as a whole, or a so-called pseudorotation. The occurrence of pseudorotation-based dynamics in CTMHs was recently described by Tagaki et al.[13] It involves the swapping of H atom positions by bond angle changes. To elucidate this question, we plotted the H–TM–H bond angles for the various centers of complexes in the simulation cell. Figures S12 – S15 show the summary of this analysis. It confirms the finding of Tagaki et al. that for complexes with high coordination numbers (here FeH_7^{3-}) H atoms perform swaps, i.e. the complexes undergo pseudorotation. This process is actually active already at 300 K. At the same time, CoH_6^{3-} units rarely display pseudorotation but rather undergo conventional reorientational dynamics (i.e. very rare change of H–TM–H bond angles) even at 1000 K.

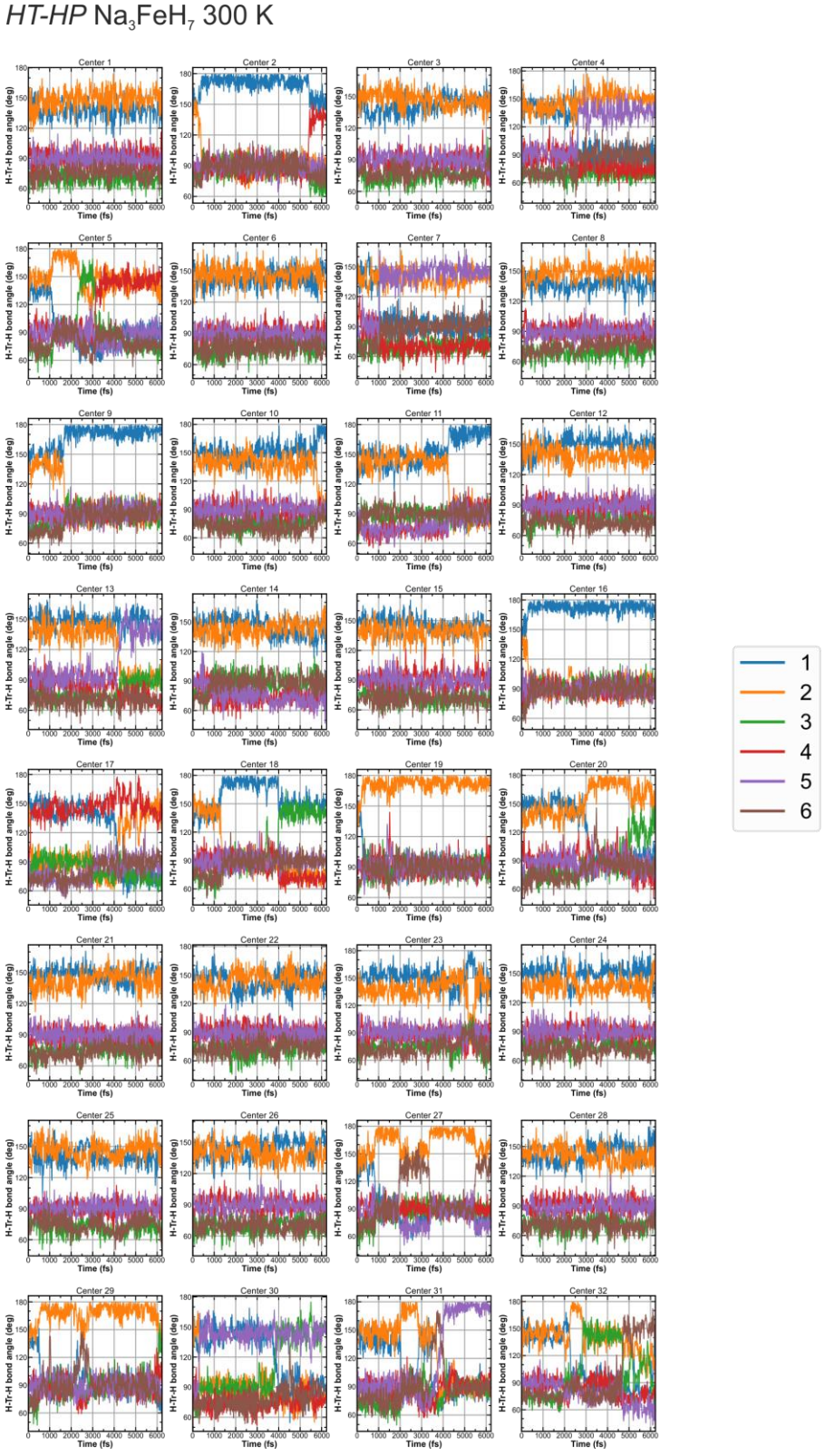

Figure S12. Time-dependent variation of H–TM–H_m (TM = Fe, Co) bond angles in *HT-HP* Na_3FeH_7 at 300 K for all 32 complexes in the simulation cell.

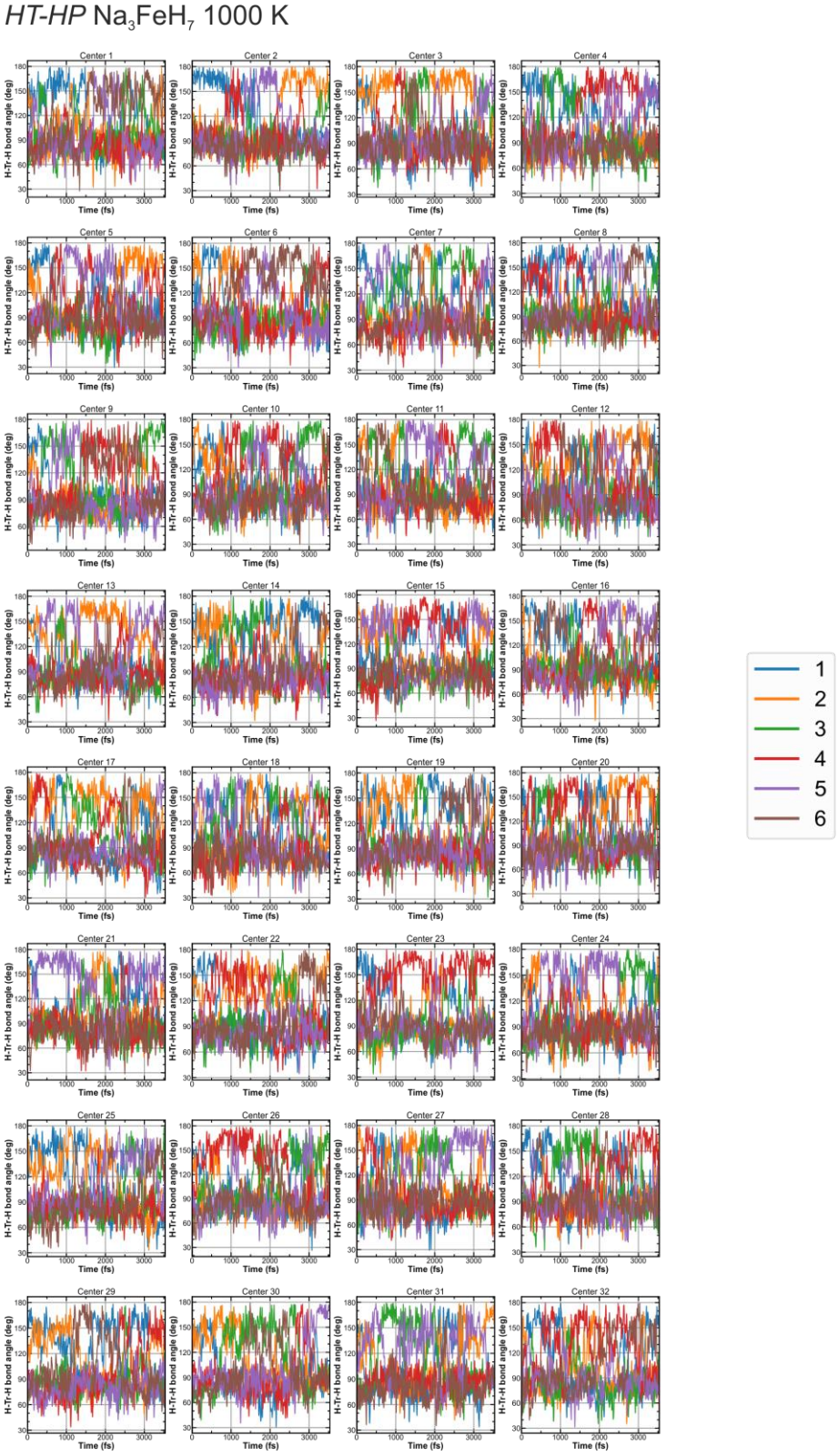

Figure S13. Time-dependent variation of H–TM–H_m (TM = Fe, Co) bond angles in *HT-HP* Na_3FeH_7 at 1000 K for all 32 complexes in the simulation cell.

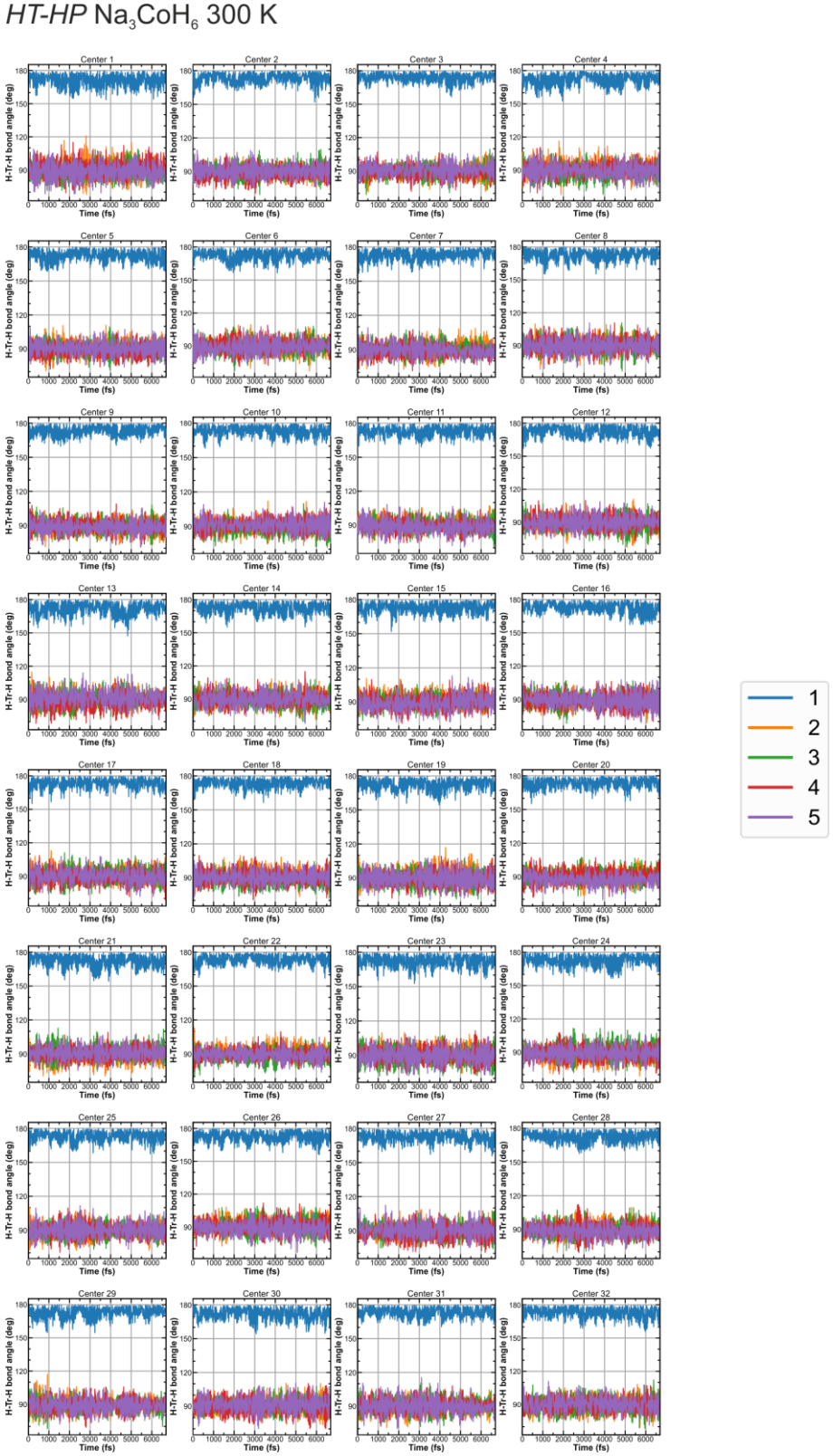

Figure S14. Time-dependent variation of H–TM–H_m (TM = Fe, Co) bond angles in *HT-HP* Na_3CoH_6 at 300 K for all 32 complexes in the simulation cell.

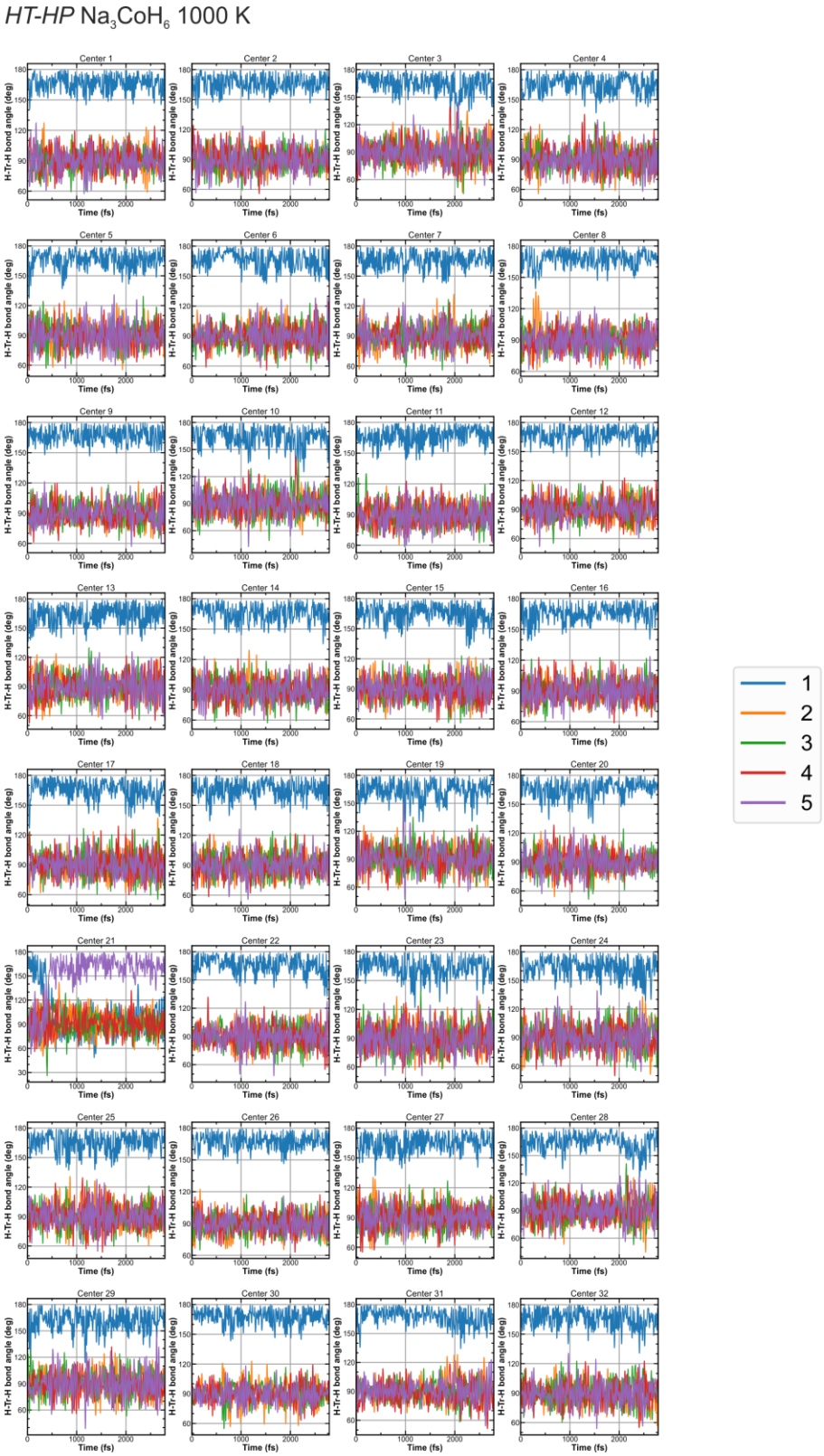

Figure S15. Time-dependent variation of H–TM–H_m (TM = Fe, Co) bond angles in *HT-HP* Na_3CoH_6 at 1000 K for all 32 complexes in the simulation cell.

3. Electronic structure calculations

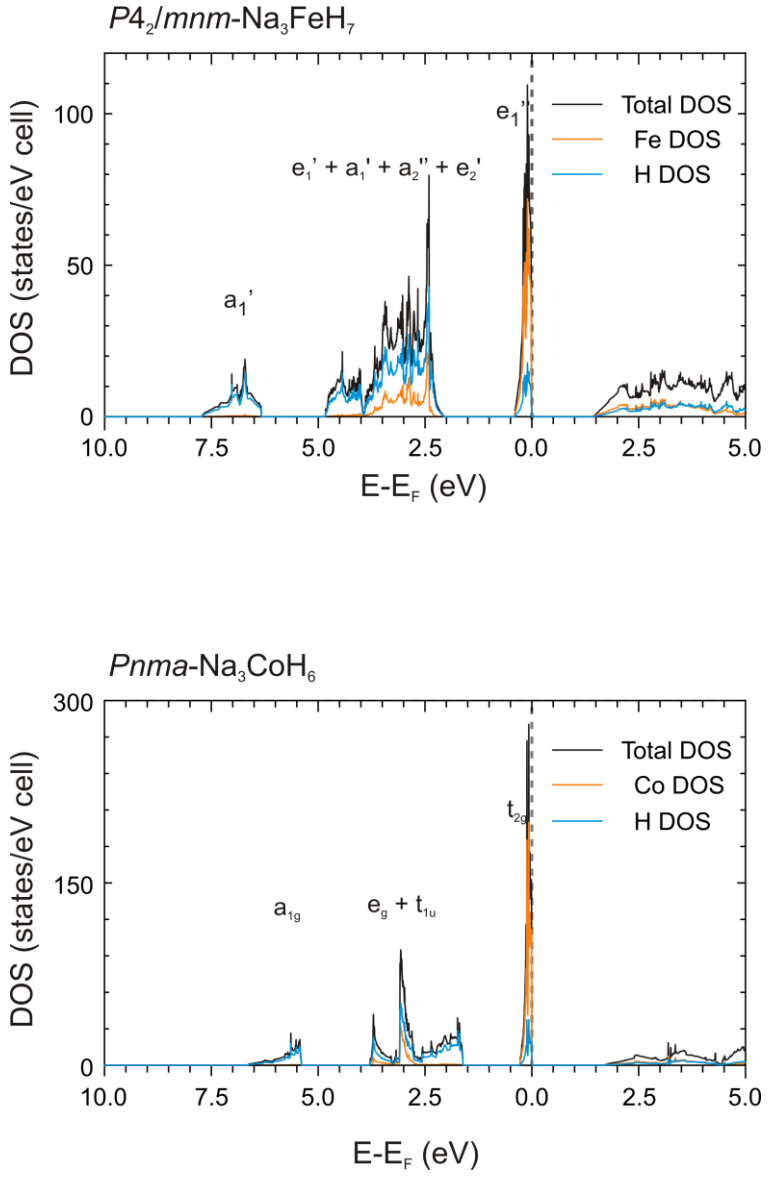

Figure S16. Electronic density of states (DOS) of *LP* $Na_3(TM)H_n$ at the equilibrium volume corresponding to ambient pressure. The bands are assigned to symmetry species according to idealized pentagonal bipyramidal complexes (D_{5h}, FeH_7^{3-}) and octahedral complexes (O_h, CoH_6^{3-}), indicating 7 Fe–H σ-bonding orbitals and 2 non-bonding, d-based, orbitals for Na_3FeH_7, and 6 Co–H σ-bonding orbitals and 3 narrow non-bonding, d-based, orbitals for Na_3CoH_6. The non-bonding orbitals express as very narrow bands. (Total DOS: black line, TM-partial DOS: orange line, H-partial DOS: blue line. Energy is plotted with respect to the energy of the highest occupied level, E_F).

4. Phonon calculations

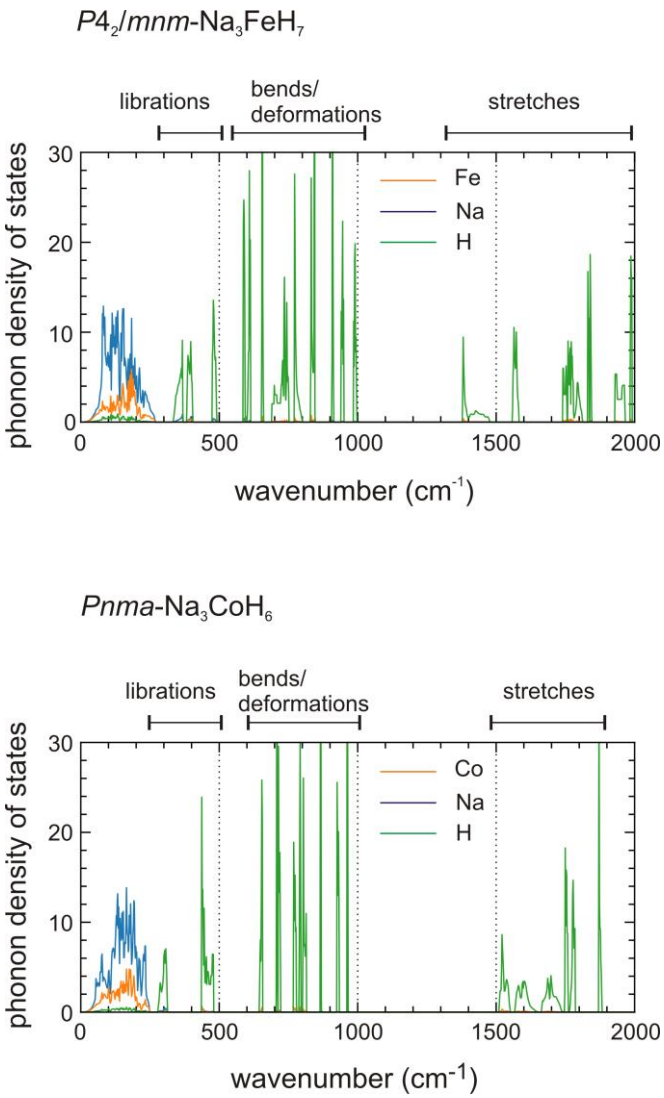

Figure S17. Phonon density of states (pDOS) of *LP* $Na_3(TM)H_n$ at the equilibrium volume corresponding to ambient pressure. The pDOS is partitioned into atomic contributions of H, Na, and TM. Typically, the vibrational properties of CTMHs are rather easy to interpret: internal modes associated with vibrations of the complex anion, i.e. TM–H stretching and bending, are clearly separated from the external (lattice) modes, *viz.* libration and translation, arising from the crystal structure. For Na_3FeH_7 (Z = 4) with pentagonal bipyramidal FeH_7 moieties, stretching (28) and bending modes (44) are in the regions 1400–2000 cm^{-1} and 600–1000 cm^{-1}, respectively. For Na_3CoH_6 (Z = 4) with octahedral CoH_6 units, stretching (24) and bending modes (36) are in the regions 1500–1900 cm^{-1} and 600–1000 cm^{-1}, respectively, which is similar to Mg_2FeH_6.[14] For Na_3FeH_7 librations (12) are in a range 330–390 cm^{-1} and for Na_3CoH_6 in a range 440–455 cm^{-1}. For both CTMHs translation bands accounting for displacements of complexes and cations are below 250 cm^{-1}.

REFERENCES

(1) Guignard, J.; Crichton, W. A. The Large Volume Press Facility at ID06 Beamline of the European Synchrotron Radiation Facility as a High Pressure-High Temperature Deformation Apparatus. *Rev. Sci. Instrum.* **2015**, *86* (8), 085112.

(2) Nylén, J.; Sato, T.; Soignard, E.; Yarger, J. L.; Stoyanov, E.; Häussermann, U. Thermal Decomposition of Ammonia Borane at High Pressures. *J. Chem. Phys.* **2009**, *131* (10), 104506.

(3) Antonov, V. E.; Baier, M.; Dorner, B.; Fedotov, V. K.; Grosse, G.; Kolesnikov, A. I.; Ponyatovsky, E. G.; Schneider, G.; Wagner, F. E. High-Pressure Hydrides of Iron and Its Alloys. *J. Phys.: Condens. Matter* **2002**, *14* (25), 6427.

(4) Fukai, Y.; Mori, K.; Shinomiya, H. The Phase Diagram and Superabundant Vacancy Formation in Fe–H Alloys under High Hydrogen Pressures. *J. Alloys Compd.* **2003**, *348* (1–2), 105–109.

(5) Spektor, K.; Crichton, W. A.; Filippov, S.; Klarbring, J.; Simak, S. I.; Fischer, A.; Häussermann, U. Na–Ni–H Phase Formation at High Pressures and High Temperatures: Hydrido Complexes $[NiH_5]^{3-}$ Versus the Perovskite $NaNiH_3$. *ACS Omega* **2020**, *5* (15), 8730–8743.

(6) Antonov, V. E.; Antonova, T. E.; Baier, M.; Grosse, G.; Wagner, F. E. On the Isomorphous Phase Transformation in the Solid f.c.c. Solutions Co–H at High Pressures. *J. Alloys Compd.* **1996**, *239* (2), 198–202.

(7) Fukai, Y.; Yokota, S.; Yanagawa, J. The Phase Diagram and Superabundant Vacancy Formation in Co–H Alloys. *J. Alloys Compd.* **2006**, *407* (1), 16–24. h

(8) Bronger, W.; Sommer, T.; Auffermann, G.; Müller, P. New Alkali Metal Osmium- and Ruthenium Hydrides. *J. Alloys Compd.* **2002**, *330–332*, 536–542.

(9) Bronger, W.; Gehlen, M.; Auffermann, G. Na_3RhH_6, Na_3IrH_6 und Li_3IrH_6, neue komplexe Hydride mit isolierten $[RhH_6]^{3-}$ und $[IrH_6]^{3-}$-Oktaedern. *J. Alloys Compd.* **1991**, *176* (2), 255–262.

(10) Le Bail, A.; Duroy, H.; Fourquet, J. L. Ab-Initio Structure Determination of $LiSbWO_6$ by X-Ray Powder Diffraction. *Mater. Res. Bull.* **1988**, *23* (3), 447–452.

(11) Petříček, V.; Dušek, M.; Palatinus, L. Crystallographic Computing System JANA2006: General Features. *Z. Kristallogr. - Cryst. Mater.* **2014**, *229* (5), 345–352.

(12) Palatinus, L.; Chapuis, G. SUPERFLIP – a Computer Program for the Solution of Crystal Structures by Charge Flipping in Arbitrary Dimensions. *J. Appl. Crystallogr.* **2007**, *40* (4), 786–790.

(13) Takagi, S.; Ikeshoji, T.; Sato, T.; Orimo, S. Pseudorotating Hydride Complexes with High Hydrogen Coordination: A Class of Rotatable Polyanions in Solid Matter. *Appl. Phys. Lett.* **2020**, *116* (17), 173901.

(14) Parker, S. F. Spectroscopy and Bonding in Ternary Metal Hydride Complexes—Potential Hydrogen Storage Media. *Coord. Chem. Rev.* **2010**, *254* (3–4), 215–234.